

Reconciling the differences between top-down and bottom-up estimates of nitrous oxide emissions for the U.S. Corn Belt

T. J. Griffis,¹ X. Lee,^{2,3} J. M. Baker,⁴ M. P. Russelle,⁴ X. Zhang,⁵ R. Venterea,⁴ and D. B. Millet¹

Received 27 March 2013; revised 30 May 2013; accepted 3 July 2013.

[1] Nitrous oxide (N₂O) is a greenhouse gas with a large global warming potential and is a major cause of stratospheric ozone depletion. Croplands are the dominant source of N₂O, but mitigation strategies have been limited by the large uncertainties in both direct and indirect emission factors (EFs) implemented in “bottom-up” emission inventories. The Intergovernmental Panel on Climate Change (IPCC) recommends EFs ranging from 0.75% to 2% of the anthropogenic nitrogen (N) input for the various N₂O pathways in croplands. Consideration of the global N budget yields a much higher EF ranging between 3.8% and 5.1% of the anthropogenic N input. Here we use 2 years of hourly high-precision N₂O concentration measurements on a very tall tower to evaluate the IPCC bottom-up and global “top-down” EFs for a large representative subsection of the United States Corn Belt, a vast region spanning the U.S. Midwest that is dominated by intensive N inputs to support corn cultivation. Scaling up these results indicates that agricultural sources in the Corn Belt released 420 ± 50 Gg N (mean ± 1 standard deviation; 1 Gg = 10^9 g) in 2010, in close agreement with the top-down estimate of 350 ± 50 Gg N and 80% larger than the bottom-up estimate based on the IPCC EFs (230 ± 180 Gg N). The large difference between the tall tower measurement and the bottom-up estimate implies the existence of N₂O emission hot spots or missing sources within the landscape that are not fully accounted for in the IPCC and other bottom-up emission inventories. Reconciling these differences is an important step toward developing a practical mitigation strategy for N₂O.

Citation: Griffis, T. J., X. Lee, J. M. Baker, M. P. Russelle, X. Zhang, R. Venterea, and D. B. Millet (2013), Reconciling the differences between top-down and bottom-up estimates of nitrous oxide emissions for the U.S. Corn Belt, *Global Biogeochem. Cycles*, 27, doi:10.1002/gbc.20066.

1. Introduction

[2] The United States Corn Belt is one of the most intensively managed agricultural regions in the world. It is a major player in terms of global food and fiber production, and recent changes in the U.S. Energy Policy Act have placed greater demands on the region for biofuel [Donner

and Kucharik, 2008]. Soybean and corn are cultivated in approximately 60 million ha of the land surface—an area greater than the entire State of California. The dominant form of new nitrogen (N) entering the cropland each year is from synthetic N fertilizers (primarily urea and anhydrous ammonia), in the amount of approximately 5.0 Tg N in 2010 (1 Tg = 10^{12} g) (Table S1, supporting information). Live-stock production within the region is also significant with an estimated population of 7.4 million animals excreting 2.7 Tg N per year in the form of manure. Measured N₂O emissions from the Corn Belt are large and in many cases offset gains associated with carbon sequestration [Robertson *et al.*, 2000; Wagner-Riddle *et al.*, 2007; Bavin *et al.*, 2009]. Developing mitigation strategies for N₂O is a critical environmental challenge as pressure mounts on our agricultural ecosystems to deliver more products to a burgeoning population and as global synthetic N production is forecasted to reach a staggering 112.9 Tg N by 2015 [Erisman *et al.*, 2008].

[3] The episodic nature and high spatial variability associated with N₂O emissions make them difficult to measure, model, and forecast [Wagner-Riddle *et al.*, 2007; Smith and Dobbie, 2001; Groffman *et al.*, 2009]. Small static chamber observations still provide the main form of flux information [Rochette and Eriksen-Hamel, 2008] and process investigation for developing emission factors (EFs) in bottom-up

Additional supporting information may be found in the online version of this article.

¹Department of Soil, Water, and Climate, University of Minnesota, Saint Paul, Minnesota, USA.

²School of Forestry and Environmental Studies, Yale University, New Haven, Connecticut, USA.

³Yale-NUIST Center on Atmospheric Environment, Nanjing University of Information Science and Technology, Nanjing, China.

⁴USDA-ARS and Department of Soil, Water, and Climate, University of Minnesota, Saint Paul, Minnesota, USA.

⁵Woodrow Wilson School of Public and International Affairs, Princeton University, Princeton, New Jersey, USA.

Corresponding authors: T. J. Griffis, Department of Soil, Water, and Climate, University of Minnesota, Saint Paul, MN 55108, USA. (timgriffis@umn.edu)

Xuhui Lee, School of Forestry and Environmental Studies, Yale University, 195 Prospect Street, New Haven, CT 06511, USA. (xuhui.lee@yale.edu)

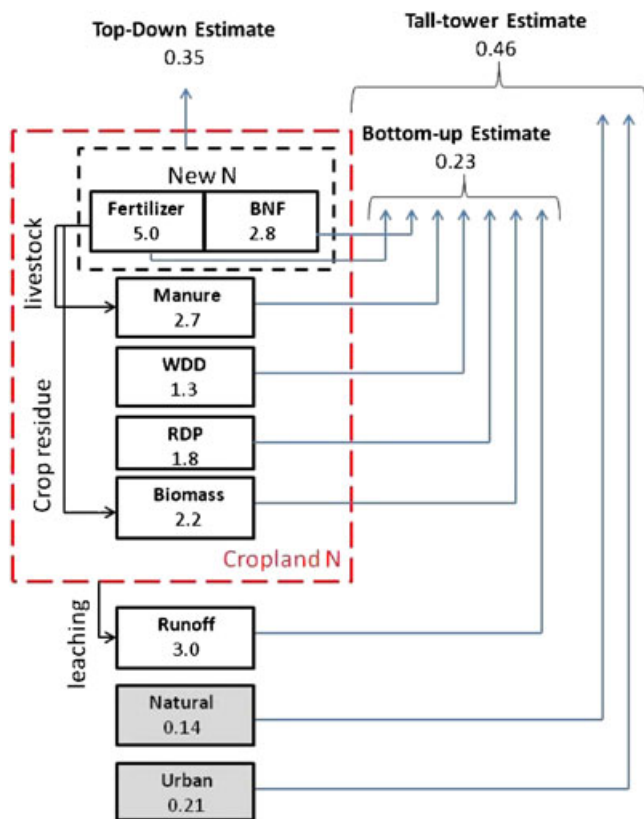


Figure 1. Nitrogen flows in the Corn Belt. Values in solid boxes represent N pools (Tg N y^{-1}). Values in shaded boxes represent N₂O-N fluxes (Tg N y^{-1}). BNF: biological nitrogen fixation; WDD: wet and dry nitrogen deposition; RDP: agricultural nitrogen redeposition.

inventories such as the Intergovernmental Panel on Climate Change (IPCC). Emission factors are used to estimate N₂O emissions from the various pathways associated with anthropogenic N inputs. The N₂O emissions are estimated by multiplying the N inputs by the EFs for each pathway. The IPCC EFs range from 0.75% to 2% with uncertainties for some EFs approaching 50-fold because of a severe limitation in observational data collected at the appropriate spatial and temporal scales [De Klein *et al.*, 2006; Outram and Hiscock, 2012]. On the other hand, consideration of the global N budget yields a much higher EF ranging between 3.8% and 5.1%, which has been shown to provide an excellent fit to the observed annual variations in global N₂O concentrations since the beginning of the anthropogenic N perturbation (ca 1860) [Crutzen *et al.*, 2008; Smith *et al.*, 2012].

[4] The bottom-up methodologies have been shown to have large uncertainties (i.e., greater than 100% for agricultural emissions) [Mosier *et al.*, 1998] and have been shown to severely underestimate N₂O emissions at the regional to continental scales [Kort *et al.*, 2008; Miller *et al.*, 2012], raising concerns over their usefulness for forecasting N₂O emissions, implementing appropriate mitigation strategies, and evaluating the effectiveness of mitigation efforts. Recently, Kort *et al.* [2008] combined aircraft flask sampling and Lagrangian particle dispersion modeling to provide a top-down constraint on N₂O emissions for North America. In their analyses, the aircraft flask sampling was limited to

May through June, 2003. Their optimization and estimate of the surface N₂O flux revealed a significant bias compared with two common bottom-up inventories (EDGAR, Emission Database for Global Atmospheric Research and GEIA, Global Emission Inventory Activity), with the inventories yielding significantly lower emission estimates by as much as threefold. Miller *et al.* [2012] advanced this approach by using near-continuous hourly N₂O tall tower data (recorded May–October, 2004 from outside of the Corn Belt in northern Wisconsin at the LEF tall tower) and supporting daily (once a day flask measurements in 2008) observations from four tall towers in the U.S. to provide better spatial and temporal boundary conditions for the inversion. Their analyses revealed strong seasonal and spatial patterns across the U.S. with the largest fluxes (1 to $2 \text{ nmol m}^{-2} \text{ s}^{-1}$) observed in June from the central U.S. Corn Belt. They also concluded that EDGAR and GEIA were biased low. However, we should note that Corazza *et al.* [2011] found relatively good agreement between their inverse modeling and bottom-up approach for northwest and eastern Europe.

[5] It is acknowledged that some of the differences between the top-down and bottom-up EFs can be explained by the different bases used to calculate the total emission. In the former, the basis for the emission calculation is the total reactive N that enters the biosphere through biological N fixation (BNF) and application of synthetic fertilizer [Crutzen *et al.*, 2008; Smith *et al.*, 2012], estimated to be 7.8 Tg N for the Corn Belt (Figure 1). In the latter, the N pool is divided into new [BNF, fertilizer, WDD (wet and dry N deposition), and RDP (N redeposition from agricultural sources)] and recycled components (manure and biomass) in the cropland and the component that has leached out of the system. The smaller EFs are compensated somewhat by the fact that some of the N is counted multiple times at various stages of the N cycle as it moves through the system.

[6] To address the question of which of the two methodologies is more appropriate at the regional scale, we carried out high-precision measurements of hourly N₂O mixing ratios near-continuously for 2 years (2010–2011) on a 244 m tall tower in Minnesota, USA. These measurements are combined with atmospheric boundary layer methods to derive a regional N₂O flux in order to address four questions: (1) What is the N₂O source strength of the Corn Belt? (2) Do state-of-the-art emission inventories and the IPCC direct and indirect N₂O EFs adequately represent the sources of N₂O for the region? (3) What is the regional anthropogenic EF for the U.S. Corn Belt and how does it relate to the bottom-up (IPCC) and top-down (global) perspectives? and (4) Are the differences between top-down and bottom-up approaches real and can they be reconciled?

2. Methodology

2.1. Study Area

[7] The tall tower trace gas observatory (TGO, Minnesota Public Radio communications tower, KCMP) is located approximately 25 km to the south of Minneapolis–St. Paul ($44^{\circ}41'19''\text{N}$, $93^{\circ}4'22''\text{W}$; 290 m ASL) at the University of Minnesota, Rosemount Research and Outreach Center (RROC). Two field-scale micrometeorological stations are also located at RROC within about 3 km of the tall tower and

have been part of the AmeriFlux network since 2004 [Baker and Griffis, 2005].

[8] Presettlement vegetation history within the tall tower flux footprint was upland dry prairie [Marschner, 1974]. Significant production of wheat, oats, corn, and potato within the region occurred as early as 1860 according to the Minnesota State Agricultural Census Data, Dakota County Historical Society. Today, land use within the vicinity of the tall tower is dominated by agriculture. For the purpose of all tall tower flux calculations, we have filtered the data according to wind direction (accepting the wind sector from 30° to 290°) to remove the urban influence of the Minneapolis-Saint Paul metropolitan area. Based on LANDSAT TM image analysis, ground truthing, and results from the USDA-NASS Crop DATA Layer (CDL) product for 2010/2011, land use consists of approximately 24% corn, 15% soybean, 6% other crop, 17% grassland, 18% woodland, 6% wetland, 4% open water, and 10% developed land within 50 km of the tall tower.

[9] Here we define the Corn Belt by those states with significant corn/soybean land use. These states include: Illinois, Indiana, Iowa, Minnesota, Missouri, Ohio, South Dakota, and Wisconsin. The total area is estimated at 148 million ha. Overall, agriculture represents approximately 40% of the land use—similar to that in the vicinity of the tall tower.

2.2. Tall Tower N₂O Measurements

[10] Tall tower N₂O and CO₂ mixing ratios were measured simultaneously using a tunable diode laser technique (TGA100A, Campbell Scientific Inc., Logan, Utah, USA). The TDL was operated in dual-ramp mode with N₂O and CO₂ measured at wave numbers 2243.760 and 2243.585, respectively. The TDL was housed at the base of the tall tower in a temperature-controlled building. Calibrations were performed hourly using a zero and span gas for N₂O and a zero and two-span gases for CO₂. The span gases were traceable to the National Oceanic and Atmospheric Administration-Earth System Research Laboratory (NOAA-ESRL). Our NOAA-ESRL N₂O gold standard (Cylinder #CA07980) concentration was 324.30 ± 0.09 ppb. The hourly TDL calibration precision was estimated using the Allan variance technique [Werle *et al.*, 1993] and was typically 0.50 ppb and 0.1 ppm for N₂O and CO₂, respectively.

[11] Air from the tall tower was sampled from inlets at approximately 32, 56, 100, and 185 m. Air was pulled continuously through each of the inlets to the base of the tower and then subsampled at three SLPM using a custom designed manifold. The air sampling and calibration consisted of the following sampling sequence where each inlet was sampled for 15 s: ultra zero air; CO₂ span 1; N₂O span; CO₂ span 2; 185 m inlet; 100 m inlet; 56 m inlet; and 32 m inlet. The air samples were dried prior to analysis using a Nafion dryer. All of the calibrated data were then block averaged into hourly values. Further details regarding the tall tower sampling and calibration scheme can be found in the supporting information of Griffis *et al.* [2010].

2.3. Boundary Layer N₂O Budgets

[12] To provide a top-down constraint on regional N₂O emissions, we have applied three boundary layer approaches including the nocturnal boundary layer (NBL), modified Bowen ratio (MBR), and equilibrium boundary layer (EBL)

techniques. Because each approach has its inherent limitations and uncertainties, we derive an ensemble estimate to arrive at a robust top-down constraint. The NBL method has been used extensively in the literature [Denmead *et al.*, 1996; Eugster and Siegrist, 2000; Pattey *et al.*, 2002]. The approach assumes that the stable NBL can be treated as a large virtual chamber, and the derived flux has a source footprint on the order of several tens of kilometers. The top of the virtual chamber is essentially defined by the development of a strong temperature inversion and the presence of a nocturnal jet stream, which typically develop at a height below 300 m. Our tall tower sonic anemometry data (100 and 185 m levels) show that nighttime wind speed at these heights are greater than surface values and typically peak during the night under stable conditions with values on the order of 5 m s⁻¹. Assuming horizontal advection is negligible, the budget equation can be written as [Denmead *et al.*, 1996],

$$F_{\text{NBL}} = \int_0^h \rho \frac{dc}{dt} dh \quad (1)$$

where ρ is the molar density of dry air, dc/dt is the change in N₂O mixing ratio during the night, and h is the height of the nocturnal boundary layer. Here, dc/dt is determined from linear regression during the nighttime (2000 to 0500 LST) and a 95% significance level was used to quality control dc/dt . Since the NBL depth was not measured directly, we estimated it based on the simple, but robust parameterization of Arya [1981],

$$h = 0.142 \frac{u_*}{f_c} \quad (2)$$

where u_* is friction velocity measured in the surface layer and f_c is the Coriolis parameter. The calculated mean height of the NBL in 2010 and 2011 was 204 and 231 m, respectively. The NBL N₂O flux data were filtered using a threshold of 3σ .

[13] The NBL budget estimate for CO₂ was calculated using the same method for N₂O and compared to eddy covariance flux measurements near the tall tower as a test of the methodology. The seasonal patterns and magnitude of the fluxes were in excellent agreement between both approaches (Figure S1, supporting information). The mean annual CO₂ flux computed from the NBL and eddy covariance approach was 2.7 $\mu\text{mol m}^{-2} \text{s}^{-1}$ and 3.3 $\mu\text{mol m}^{-2} \text{s}^{-1}$ in 2010 and 2.7 $\mu\text{mol m}^{-2} \text{s}^{-1}$ and 2.8 $\mu\text{mol m}^{-2} \text{s}^{-1}$ in 2011. The differences among these estimates are well within the uncertainty of each method.

[14] Second, we calculated nighttime and daily (day and night) N₂O fluxes using the MBR approach. In this case, CO₂ was used as the tracer with the CO₂ flux measured by eddy covariance within the vicinity of the tall tower [Baker and Griffis, 2005; Griffis *et al.*, 2010] and the CO₂ concentration gradients were measured simultaneously at the tall tower using the same inlets and TDL described above. In this approach we assume similarity regarding the diffusivity and transport of each scalar and assume the eddy covariance CO₂ flux is representative of regional nighttime values. The N₂O flux was computed from,

$$F_{\text{MBR}} = F_c \frac{dc_1/dz}{dc_2/dz} = F_c \frac{dc_1}{dc_2} \quad (3)$$

where F_c is the eddy CO₂ flux, and dc_1/dz and dc_2/dz represent the vertical gradients of N₂O and CO₂, and were

determined using linear regression. Here we used a 95% significance level to quality control the gradient estimates. The nighttime flux was determined using the same time interval as defined above.

[15] Finally, we used the EBL approach [Betts, 2000; Betts et al., 2004; Helliker et al., 2004; Desai et al., 2010] to estimate the N₂O flux at monthly intervals. In this approach, the diurnal dynamics of the convective boundary layer and nocturnal boundary layer are ignored based on the assumption that, at longer time scales (on the order of a few days to months), the boundary layer is in statistical equilibrium and the large scale atmospheric processes dominate. This idea was first demonstrated for the surface heat and water budgets [Betts, 2000] and has been used increasingly for quantifying regional scale CO₂ fluxes [Betts et al., 2004; Helliker et al., 2004; Desai et al., 2010]. The derived flux has a source footprint on the order of several hundreds of kilometers. Here we applied the same approach to N₂O where over the long term, the surface flux is in steady state with the troposphere exchange. We estimated the monthly N₂O emission from,

$$F_{\text{EBL}} = \int_0^h \rho \frac{dc}{dt} dh + S(C_t - C_m) \quad (4)$$

where F_{EBL} is the surface flux, S represents the subsidence of air from the free troposphere into the boundary layer (units of mol m⁻² s⁻¹ and positive toward the surface), C_t and C_m represent the mixing ratios of N₂O in the free atmosphere and mixed layer, respectively. Here we ignore horizontal advection, which has been shown to be negligible over these long averaging periods [Williams et al., 2011]. Despite the simplicity of this approach, the variables S and C_t are challenging to quantify on a near-continuous basis. Here we have used the North American Regional Reanalysis data sets (<http://esrl.noaa.gov>) and background N₂O concentration measurements made from North American NOAA Cooperative Global Air Sampling Network stations-Niwot Ridge and Mauna Loa. In our analysis we determined the vertical subsidence at the 700 hPa pressure level. We have determined all of the variables in equation (4) using mean monthly values. However, given the noise in S , we have estimated it based on the ensemble of 5 years (2007 to 2011).

2.4. Source Footprint Within the Corn Belt

[16] While it would be ideal to have multiple tall towers with high frequency N₂O measurements within the Corn Belt, we are limited to extrapolating the measurements from TGO/KCMP to the region. The source footprints of the NBL, MBR, and EBL methods are expected to range from about 10 to 100 km. Our data and analyses, therefore, are representative of a relatively broad portion of the northern U.S. Corn Belt. Based on LANDSAT TM image analysis, ground truthing, and results from the USDA-NASS Crop DATA Layer (CDL) product for 2010/2011, land use statistics are consistent at spatial scales extending out to about 150 km from the tall tower [Griffis et al., 2010; Zhang et al., 2013]. A detailed nitrogen survey conducted for Minnesota [Beirman et al., 2012] found that the typical N application rate for corn in Minnesota was 157 kg N ha⁻¹ (range of 145 to 164 kg ha⁻¹) and was in excellent agreement with the average N application rate (143 kg N ha⁻¹) used across the Corn Belt (see supporting information). Estimates of corn yield for Minnesota (156 bushels per acre in 2011) are also

within 6% of the U.S. Corn Belt average of 147 bushels per acre [USDA-NASS, 2013]. There is also strong coherence in the behavior of hourly CO₂ mixing ratios among nine tall towers located in the Upper Midwest Corn Belt [Miles et al., 2012]. The large draw-down in growing season daytime CO₂ among these sites supports the assumption that the Minnesota tall tower is representative of this agricultural landscape. Finally, based on the Stochastic Time-Inverted Lagrangian Transport (STILT) model [Lin et al., 2003], we estimated the peak sensitivity of the NBL concentration footprint (185 m level) to be approximately 120 km for a typical night (Figure S2, supporting information).

2.5. Global N₂O Data Sets

[17] Hourly N₂O concentration data from NOAA-ESRL Cooperative Global Air Sampling Network stations (background sites) were used to support our investigation (www.esrl.noaa.gov/gmd/). These stations included Niwot Ridge, Colorado, USA, and Mauna Loa, Hawaii, USA, Barrow, Alaska, USA, Summit Greenland, and the South Pole. These data have a reported concentration precision of 0.3 to 0.6 ppb. Note that all of the N₂O concentration and flux data (tall tower, chamber, and background sites) reported in this study are traceable to the NOAA-ESRL scale.

2.6. Wavelet Analysis

[18] The tall tower and global N₂O concentration data were analyzed using wavelet decomposition in order to better understand the hourly variations and to extract longer-term (seasonal) variations from each of the data sets. We used the traditional and relatively simple Haar wavelet to decompose the original N₂O signals into their approximate and detailed components/coefficients using a five-level decomposition. All analyses were conducted using the MATLAB Wavelet Toolbox (MATLAB V7.5, The Mathworks Inc., MA, USA).

2.7. Chamber Measurements

[19] We used a flow-through non-steady state chamber system coupled to a second TDL system to measure soil N₂O fluxes during 2010 and 2011. Technical details of the chamber system have been reported in previous papers [Fassbinder et al., 2012; Fassbinder et al., 2013]. Here we note that in 2010, three chambers were placed within a small experimental corn plot (20 m × 20 m) established within a large 40 ha soybean field. Three other chambers were placed within the soybean field. In 2011, all six chambers were placed within a corn field. Fluxes from each chamber were determined using a measurement period of 15 min and each chamber was sampled every 90 min. In spring 2012 we used a modified chamber system to measure N₂O fluxes from drainage ditches and shallow open water sources connected to agricultural activity. Further, we have examined chamber measurements conducted by other researchers within the Corn Belt to determine typical N₂O emissions from agricultural lands and associated water pathways.

2.8. Bottom-up N₂O Emission Estimates

[20] The IPCC EF formulae and emission guidelines [De Klein et al., 2006] were applied to the Corn Belt using best estimates of the key N inputs (Table S1, supporting

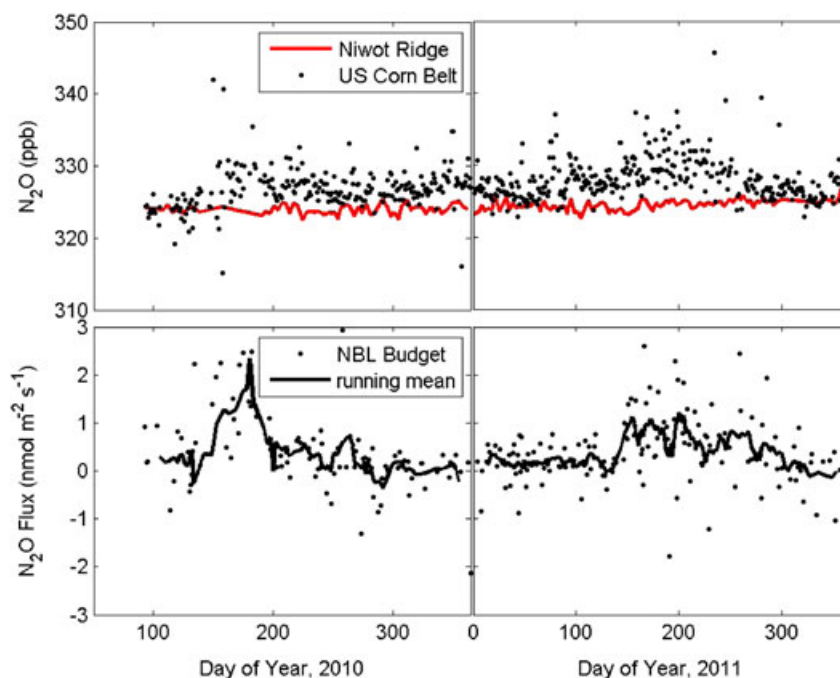


Figure 2. Tall tower atmospheric observations in the Corn Belt. (top) Daily N₂O mixing ratio measured at a height of 100 m above the ground at the Rosemount Research and Outreach Center, University of Minnesota and background N₂O mixing ratio measured at Niwot Ridge, a NOAA-ESRL Cooperative Global Air Sampling Network Station. The Niwot Ridge data have been smoothed using a 3 day running mean. (bottom) Time series of the regional N₂O flux derived from the nocturnal boundary layer budget method. A running mean of 7 days is shown as the solid black line.

information). The IPCC methodology defines anthropogenic “direct” N₂O emissions from soils where N has been added in the form of synthetic/organic fertilizer, crop residue, and sewage sludge, or where soil N mineralization has changed as a consequence of land use activity. The “indirect” emission of N₂O is related to volatilization products (NH₃, and NO_x) that are deposited back to the soil and thereby contribute to N₂O emissions. Indirect sources include leaching and runoff of N from fertilizer, manure, and residue, which leads to N₂O emission at significant distances from its origin.

[21] We have estimated the indirect N₂O emissions as follows: First, we represent the volatilization indirect pathway based on wet and dry N deposition into the region and also consider the redeposition of local N. Second, we have applied the IPCC equation 11.10 to estimate N₂O emissions associated with leaching and runoff. The IPCC direct EFs used in this study include the following: For fertilizer additions (synthetic/organic), the recommended factor is 0.01 with an uncertainty range of 0.003 to 0.03. For manure application (including cattle, swine, horses, sheep, chickens) the recommended factor is 0.02 (0.007 to 0.06). The IPCC indirect EFs are as follows: For N₂O emissions associated with volatilization, the EF is 0.01 (0.002 to 0.05). For leaching and runoff in nonarid regions the leaching/runoff scaling factor is 0.3 (0.1 to 0.8) and the EF is 0.0075 (0.0005 to 0.025).

[22] To estimate the uncertainty associated with our IPCC bottom-up emission estimate, we conducted a Monte Carlo simulation. In this simulation we assumed a normal probability distribution for each EF using the uncertainty ranges provided above. The uncertainty in the bottom-up emission estimate was then determined as one standard deviation

from a sample population of 10,000 simulations. For comparison, we also used two emission databases (EDGAR, version V4.2; GEIA) to estimate anthropogenic emissions of N₂O for the region [<http://edgar.jrc.ec.europa.eu>, 2011; Bouwman *et al.*, 1995]. As shown below, excellent agreement was observed between EDGAR and our IPCC estimates, with both significantly higher than GEIA.

3. Results and Discussion

3.1. Spatio-Temporal Variations in N₂O Concentrations

[23] For context, we begin our analysis with a discussion of the recent N₂O data from the NOAA Cooperative Global Air Sampling Network. These data are representative of background sites with no direct influence of agriculture. The mean annual N₂O concentrations measured at Niwot Ridge, Mauna Loa, Barrow Alaska, American Samoa, Summit Greenland, and the South Pole were 324.50 ± 0.77 , 324.69 ± 0.67 , 324.71 ± 0.79 , 324.11 ± 0.78 , 324.38 ± 0.83 , and 323.49 ± 0.72 ppb, respectively, in 2011 (see Figure 2 for a subsample of the time series data). Barrow Alaska and Mauna Loa exhibited the highest mean annual concentrations from 2010 to 2012. The standard deviations of these hourly values indicate that hour-to-hour fluctuations are relatively small, with maximum variations on the order of 2 to 4 ppb.

[24] The wavelet decomposition (Figure S3) shows that there is very little seasonal variation observed at any of these background sites, but rather a slow and steady increase is apparent at most sites. For instance, N₂O concentration

increased by about 0.27%, 0.31%, 0.26%, and 0.39% at Mauna Loa, Niwot Ridge, South Pole, and American Samoa sites, respectively, during 2011. An interesting feature at each of these sites is a rather flat response in the signal from DOY 1 through DOY 150, after which an increasing trend is observed. Using wavelet signal detection, we find that there is no significant influence of spring snowmelt or increasing spring temperatures on the episodic behavior of N₂O concentration nor is there a significant seasonal pattern at any of these background sites, including those located in northern terrestrial environments (Niwot Ridge and Barrow Alaska).

[25] The tall tower hourly N₂O concentrations measured at 100 m from April 2010 to April 2012 are shown in Figure 2. The mean annual N₂O concentrations were 327.32 and 327.75 ppb, respectively. The difference between these 2 years was within the uncertainty of the hourly precision (0.50 ppb). The tall tower concentration was 3.06 ppb more elevated than the atmospheric “background” value observed at Niwot Ridge, Colorado (Figure 2). This difference is 2.6 times the gradient between the two hemispheres, indicating that the Corn Belt is a strong source of N₂O and relevant at the global scale.

[26] The tall tower N₂O data also reveal strong episodic features and seasonal variations not observed at the background sites (Figures 2 and S3). The wavelet decomposition clearly shows a strong increase in N₂O concentration near the timing of spring warming/snowmelt (DOY 74, 2011). N₂O emissions during snowmelt or during freeze/thaw cycles have been reported to be significant, and it has been suggested that these events may account for up to 70% of the annual N₂O budget [Wagner-Riddle and Thurtell, 1998; Rover *et al.*, 1998]. These events are usually characterized by a large flush of N₂O when soil temperatures are near 0°C [Chen *et al.*, 1995], but subside as soil temperatures rise above 2°C. This correlates with high N₂ emission rates, which is likely due to increasing activity of N₂O reductase [Muller *et al.*, 2003]. Further, the magnitude of the flush is related to the length of the frozen period, which is quite long (often > 4 months) in southeastern Minnesota. We also observed a substantial increase in N₂O concentration during early spring 2012 (data not shown) in the absence of any significant regional snow cover from the previous winter. This was correlated with the extreme warm temperature anomaly of March 2012, with mean air temperatures 8.7°C higher than the recent 30 year normal.

[27] The wavelet decomposition also reveals that the Rosemount site exhibits a strong seasonal pattern compared to the background sites. The seasonal amplitude for the near-complete 2011 data set was approximately 5 ppb. The annual ensemble diurnal amplitude (peak to peak at 100 m, data not shown) in N₂O concentration was 1.2 ppb. The largest amplitudes, typically greater than 2.5 ppb, were observed from June through September, while nongrowing season values were about 1.0 ppb. These patterns suggest that N₂O emissions are greatest from June through September, as described in more detail below.

[28] Adipic acid production from industrial processes can cause elevated N₂O concentrations in urban areas as observed by Corazza *et al.* [2011]. However, analyses of N₂O concentrations as a function of wind direction indicate that elevated N₂O concentrations at the tall tower are

associated with southerly winds with a source footprint dominated by agriculture. There is autocorrelation among wind direction, air temperature, and N₂O concentrations at this site, however, analysis of the high temperature data (> 20°C) indicate similar patterns, suggesting that the Minneapolis-Saint Paul metropolitan area has very limited influence on the N₂O concentrations compared to agricultural sources (Figure S4). Nevertheless, to avoid the influence of urban N₂O emissions on our tall tower boundary layer budget estimates, we have eliminated time periods when the source footprint included the metropolitan area.

3.2. Top-down Constraints on N₂O Emissions

[29] The concentration data presented above were used with three boundary layer budget approaches to help constrain the regional N₂O emissions. The NBL N₂O flux shows that emissions ranged up to 2 nmol m⁻² s⁻¹ and generally peaked in June (Figure 2), corresponding to the timing of fertilizer application, warm temperatures, ample precipitation, and the emergence of agricultural crops within the region. The mean monthly NBL N₂O emissions are shown in Figure S5 and indicate that the largest fluxes were observed during the growing season, which is generally consistent with our automated soil chamber measurements (Figure S6). The mean (± the standard error) annual NBL N₂O fluxes were 0.34 ± 0.11 nmol m⁻² s⁻¹ and 0.39 ± 0.05 nmol m⁻² s⁻¹ in 2010 and 2011, respectively.

[30] The mean annual nighttime MBR N₂O estimates were in good agreement with the NBL approach and ranged from 0.42 ± 0.06 to 0.30 ± 0.04 nmol m⁻² s⁻¹ in 2010 and 2011, respectively. The mean annual daily MBR N₂O values ranged from 0.33 ± 0.06 to 0.29 ± 0.05 nmol m⁻² s⁻¹ in 2010 and 2011, respectively.

[31] The mean annual N₂O flux derived from the EBL approach was 0.42 ± 0.09 and 0.36 ± 0.09 nmol m⁻² s⁻¹ in 2010 and 2011, respectively and were in good agreement with the NBL and MBR estimates. The EBL flux estimate was very similar if Niwot Ridge or Mauna Loa was used as the background (tropospheric) values. For example, the difference in mean annual flux ranged from 0.02 to 0.01 nmol m⁻² s⁻¹ for the respective years.

[32] Overall, the three different atmospheric boundary layer methods show similar seasonal variations with correlation coefficients ranging from 0.47 to 0.80 for each of the methods. However, there are some notable differences in the monthly values. We hypothesize that some of the variability among the methods can be attributed to the differences in their source footprints. The source footprint varies among these methods from tens to hundreds of kilometers. However, some of the variability can be attributed to the uncertainties in each approach. The 2 year annual ensemble flux for all methods gives a mean value and standard deviation of 0.35 ± 0.05 nmol m⁻² s⁻¹. We also note that the growing season tall tower flux (0.51 ± 0.20 nmol m⁻² s⁻¹) is in excellent agreement with the top-down flux (0.6 nmol m⁻² s⁻¹) derived independently from atmospheric inverse modeling for this region [Miller *et al.*, 2012].

[33] Multiplying the tall tower flux by the total land area of 148 million ha gives the total annual N₂O emission of 460 ± 60 Gg N for the Corn Belt. This amount is substantial, representing more than 10% of the net global N₂O atmospheric sink [Hirsch *et al.*, 2006], confirming the important

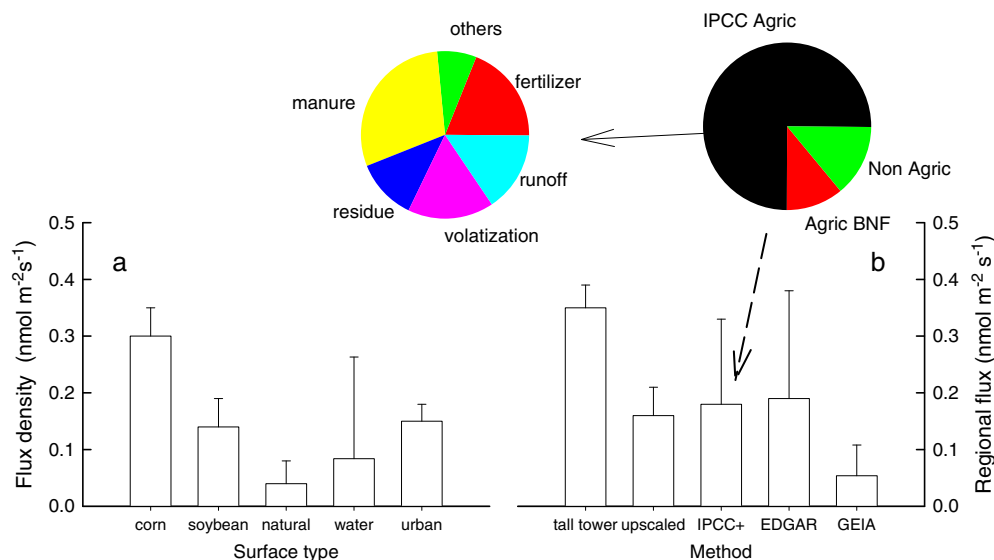


Figure 3. Comparison of N₂O flux densities. (a) Annual mean flux density for the surface types in the tall tower footprint. (b) Comparison of regional flux estimates using different methods. The figure insets show each IPCC component.

role of the U.S. Corn Belt in the global N₂O budget [Kort *et al.*, 2008; Miller *et al.*, 2012]. By subtracting the contributions from urban land and natural vegetation, based on literature values, we obtain a cropland emission of 420 ± 50 Gg N. This estimate is in good agreement with the global top-down approach proposed by Crutzen *et al.* [2008]. For example, given a mean top-down EF of 4.5%, we estimated an N₂O emission of 350 ± 50 Gg N from the Corn Belt, with the uncertainty range corresponding to the uncertainty in the top-down EF.

3.3. Bottom-Up Constraints on N₂O Emissions

[34] The IPCC bottom-up methodology yields a much smaller emission of 180 ± 170 Gg N. The uncertainty range here represents ± 1 standard deviation of the ensemble estimates generated by the Monte Carlo simulation with a distribution of the EFs for their ranges reported in IPCC. The IPCC accounting guideline excludes emissions from BNF [De Klein *et al.*, 2006]. When BNF in the Corn Belt is included, to be consistent with the top-down methodology, this bottom-up estimate increases slightly to 230 ± 180 Gg N. Further, the tall tower flux density is 2.6 and 8.8 times greater than the regional fluxes derived from EDGAR and GEIA, respectively, the two inventory data sources commonly used in atmospheric models (Figure 3b).

[35] In order to compare with anthropogenic emission estimates, we have made two flux upscaling calculations since the tower footprint encompasses additional source categories (Figure 1). In one calculation, we first compiled the flux densities for the individual land use types according to our own measurements of soil N₂O flux in corn and soybean fields within the tower footprint and the data reported in the literature for urban land, natural vegetation, and lakes (Figure 3). Next, we weighted the individual contributions by their fractional land areas. In the final step, an upward adjustment of 0.03 nmol m⁻² s⁻¹ was made to account for emissions from manure, assuming uniform distribution throughout the Corn Belt. The aggregated regional

flux computed from this method is 0.16 ± 0.05 nmol m⁻² s⁻¹ (Figure 3). In the second calculation, we added to the IPCC emission estimate contributions from urban land, natural vegetation, and biological N fixation, obtaining a regional flux of 0.19 ± 0.17 nmol m⁻² s⁻¹. Both of these upscaled fluxes are much lower than our observed tall tower flux or that derived from inverse modeling for the region [Kort *et al.*, 2008; Miller *et al.*, 2012].

3.4. Reconciling Top-Down and Bottom-Up N₂O Emissions

[36] Although the uncertainties are relatively large in both the top-down and bottom-up N₂O emission estimates, there is growing consensus from independent studies and independent approaches, that the top-down atmospheric estimates are at least twofold greater for North America and the U.S. Corn Belt [Kort *et al.*, 2008; Miller *et al.*, 2012]. Here we attempt to reconcile these differences and put forth a hypothesis regarding the role of N₂O emission hot spots from fine-scale agricultural drainage features and their potential influence on the regional budget.

[37] We have more confidence in some of the IPCC EFs than in others. For example, direct emissions resulting from synthetic N fertilizer application is a major contributor to the overall emission estimate (insets to Figure 3b), and our soil chamber measurements support the validity of the IPCC EF for this source category (Figure S6). The soil N₂O flux measured in our experimental corn field is about 1.3% of the N fertilizer application rate, consistent with the IPCC-recommended EF of 1% (0.3% to 3.0% range). Numerous other field observations also show similar ratios of the N₂O flux to the N input [Gregorich *et al.*, 2005; Stehfest and Bouwman, 2006; Millar *et al.*, 2010; Cavigelli and Parkin, 2012]. Another major source category is emission from animal manure applications. The IPCC methodology assumes an EF of 2%. Although we have not measured the EF of this source category, other studies have confirmed that the IPCC EF is within 0.7% to 6% [De Klein *et al.*, 2006]. For

leaching and runoff in nonarid regions, a scaling factor of 0.3 is used to estimate the runoff N and then an EF of 0.75% is applied. Both factors have large uncertainty. The EF has an uncertainty that ranges 50-fold (0.05% to 2.5%) and is based on only 10 studies [Outram and Hiscock, 2012] with extremely limited spatial and temporal distribution. Thus, it is likely that these previous studies missed emission hot spots, as discussed below.

[38] The tall tower flux is also greater than any of the individual flux densities considered in Figure 3a. To bring the upscaled flux into agreement with the tall tower flux would require substantial contributions from minor land use types omitted in Figure 3a. Recent investigations have identified the importance of N₂O emission associated with surface waters in agricultural land [Outram and Hiscock, 2012; Beaulieu *et al.*, 2011]. These studies have shown that despite their limited spatial extent, they are responsible for a disproportionate amount of the indirect N₂O emissions. Drainage ditches appear to be N₂O emission hot spots. Emissions from drainage ditches in an agricultural catchment in England are one order of magnitude greater than its headwater streams and are responsible for nearly 90% of the total indirect emissions [Outram and Hiscock, 2012].

[39] The N₂O emission from tile drains of a corn field near our tall tower occurred at a mean rate of 13 nmol m⁻² s⁻¹ (range 0.3–64 nmol m⁻² s⁻¹) during the early growing season, which is 40-fold greater than the flux from headwater streams in an agricultural catchment in the Corn Belt (0.35 nmol m⁻² s⁻¹) [Beaulieu *et al.*, 2008]. The flux from lakes, which are further downstream than headwater streams, is even lower (Figure 3a), suggesting that “water age”, or the time drainage water spends in waterways after it has exited cropland soil, is a critical factor controlling in situ denitrification [Peterson *et al.*, 2001]. If we attribute the difference between the top-down and the IPCC estimates solely to leaching and runoff, the EF for this source category would increase drastically to 4.0% from the nominal value of 0.75% and higher than any reported EF in the literature for these sources. That the bottom-up and the top-down emission estimates show reasonable agreement on the global scale [Del Grosso *et al.*, 2008; Smith *et al.*, 2012], but are substantially different for the Corn Belt implies compensating biases among different regions of the world.

[40] The Corn Belt has been subjected to intensive drainage in order to increase agricultural productivity. Best estimates indicate that 25% to 50% of the Corn Belt has been drained [USDA, 1987]. In drier climates where agricultural drainage is less prevalent, the associated indirect leakage mechanisms may be much weaker. Currently, land managers in the Corn Belt are not required to disclose how much of their land is tile drained or when new drainage ditches have been added. With increasingly high resolution LiDAR-derived elevation data (1 m), remote sensing, advances in geospatial analyses, and new low-cost N₂O flux chambers [Fassbinder *et al.*, 2013], it is becoming feasible to identify these drainage networks and quantify the associated fluxes. We postulate that an improved understanding of these fine-scale geographic sources is crucial to identifying hot spots and hot moments [Groffman *et al.*, 2009] and resolving the lack of closure in regional N budget studies in North America [Kort *et al.*, 2008; Miller *et al.*, 2012].

4. Conclusions

[41] Hourly N₂O observations made from a tall tower in the Upper Midwest United States were used to assess regional N₂O fluxes and EFs within the Corn Belt from 2010 to 2011. The data and analyses support the following conclusions:

[42] 1. Boundary layer budget estimates of N₂O using three different techniques ranged from 0.29 to 0.42 nmol m⁻² s⁻¹ over the 2 year period. The ensemble mean flux using these methods was 0.35 ± 0.05 nmol m⁻² s⁻¹.

[43] 2. The boundary layer budget estimates were approximately 2.6- to 8.8-fold greater than bottom-up approaches including the IPCC, EDGAR, and GEIA approaches and supports previous conclusions based on short-term inverse modeling.

[44] 3. The N₂O budget estimated by applying the top-down (global) EF of 4.5% to anthropogenic nitrogen inputs was in relatively good agreement with the tall tower regional budget assessment. These analyses, in combination with chamber observations from fine-scale agricultural drainage features, suggest that indirect emissions are poorly constrained by the bottom-up approaches.

[45] 4. Given the projected increase in regional nitrogen demand, our analyses support that N₂O emissions from the Corn Belt are likely to increase substantially. This increase may be enhanced in the Upper Midwest where hydrometeorological conditions have become wetter and drainage and stream flow have increased over the last 50 years.

[46] **Acknowledgments.** This research was supported by the United States Department of Agriculture National Institute of Food and Agriculture (NIFA/2010-65112-20528), the Ministry of Education of China (PCSIRT) and the Viola Fund of New York. We thank Matt Erickson, Joel Fassbinder, Bill Breiter, Peter Turner, and Natalie Schultz for their help in maintaining the field measurements. We also acknowledge Minnesota Public Radio (KCMP 89.3, “The Current”) and Tom Nelson for providing logistical support for this project. Finally, we thank the Dietz Brothers climbing crew for installing and maintaining our instrumentation on the KCMP tower.

References

- Arya, S. (1981), Parameterizing the height of the stable atmospheric boundary layer, *J. Appl. Meteorol.*, 20, 1192–1202.
- Baker, J. M., and T. J. Griffis (2005), Examining strategies to improve the carbon balance of corn/soybean agriculture using eddy covariance and mass balance techniques, *Agr. Forest. Meteorol.*, 128, 163–177.
- Bavin, T., T. Griffis, J. Baker, and R. Venterea (2009), Impacts of reduced tillage and cover cropping on the greenhouse gas budget of a maize/soybean rotation ecosystem, *Agric. Ecosyst. Environ.*, 134, 234–242.
- Beaulieu, J. J., *et al.* (2011), Nitrous oxide emission from denitrification in stream and river networks, *Proc. Natl. Acad. Sci. USA.*, 108(1), 214–219, doi:10.1073/pnas.1011464108.
- Beaulieu, J. J., C. P. Arango, S. K. Hamilton, and J. L. Tank (2008), The production and emission of nitrous oxide from headwater streams in the Midwestern United States, *Global Change Biol.*, 14(4), 878–894, doi:10.1111/j.1365-2486.2007.01485.x.
- Beirman, P., C. Rosen, R. Venterea, and J. Lamb (2012), Survey of nitrogen fertilizer use on corn in Minnesota, *Agr. Syst.*, 109, 43–52.
- Betts, A. (2000), Idealized model for equilibrium boundary layer over land, *J. Hydrometeorol.*, 1, 507–523.
- Betts, A. K., B. Helliker, and J. Berry (2004), Coupling between CO₂, water vapor, temperature, and radon and their fluxes in an idealized equilibrium boundary layer over land rid b-8211-2009, *J. Geophys. Res.*, 109, D18103, doi:10.1029/2003JD004420.
- Bouwman, A., K. van der Hoek, and J. Olivier (1995), Uncertainties in the global source distribution of nitrous oxide, *J. Geophys. Res.*, 100(D2), 2785–2800.
- Cavigelli, M. A., and T. B. Parkin (2012), Cropland management contribution to greenhouse gas flux: Eastern and central U.S., in *Managing*

- Agricultural Greenhouse Gases: Coordinated Agricultural Research through GRACENet to Address our Changing Climate*, edited by M. Liebig, R. Follett, and A. Franzluebbers, pp. 129–166, Academic Press, Waltham, Mass.
- Chen, Y., S. Tessier, A. F. Mackenzie, and M. R. Laverdiere (1995), Nitrous-oxide emission from an agricultural soil subjected to different freeze-thaw cycles, *Agric. Ecosyst. Environ.*, *55*(2), 123–128.
- Corazza, M., et al. (2011), Inverse modelling of European N₂O emissions: Assimilating observations from different networks, *Atmos. Chem. Phys.*, *11*(5), 2381–2398, doi:10.5194/acp-11-2381-2011.
- Crutzen, P., A. Mosier, K. Smith, and W. Winiwarter (2008), N₂O release from agro-biofuel production negates global warming reduction by replacing fossil fuel, *Atmos. Chem. Phys.*, *8*, 389–395.
- De Klein, C., R. S. A. Novoa, S. Ogle, K. A. Smith, P. Rochette, T. C. Wirth, B. G. McConkey, A. Mosier, and K. Rypdal (2006), N₂O emissions from managed soils, and CO₂ emissions from lime and urea application, in *2006 IPCC Guidelines for National Greenhouse Gas Inventories, Vol 4: Agriculture, Forestry and Other Land Use*, edited by H. S. Eggleston et al., pp. 11.11–11.54, Institute for Global Environmental Strategies (IGES), Intergovernmental Panel on Climate Change (IPCC), Kanagawa, Japan.
- Del Grosso, S., T. Wirth, S. Ogle, and W. Parton (2008), Estimating agricultural nitrous oxide emissions, *EOS T. Am. Geophys. Un.*, *89*, 529–540.
- Denmead, O., M. Raupach, F. Dunin, H. Cleugh, and R. Leuning (1996), Boundary layer budgets for regional estimates of scalar fluxes, *Glob. Change Biol.*, *2*(3), 255–264, doi:10.1111/j.1365-2486.1996.tb00077.x.
- Desai, A. R., B. R. Helliker, P. R. Moorcroft, A. E. Andrews, and J. A. Berry (2010), Climatic controls of interannual variability in regional carbon fluxes from top-down and bottom-up perspectives rid b-8211-2009, *J. Geophys. Res.-Biogeo.*, *115*, G02011, doi:10.1029/2009JG001122.
- Donner, S., and C. Kucharik (2008), Corn-based ethanol production compromises goal of reducing nitrogen export by the Mississippi River, *Proc. Natl. Acad. Sci. USA.*, *105*, 4513–4518.
- Erismann, J., M. Sutton, J. Galloway, Z. Klimont, and W. Winiwarter (2008), How a century of ammonia synthesis changed the world, *Nat. Geosci.*, *1*, 636–639.
- Eugster, W., and F. Siegrist (2000), The influence of nocturnal CO₂ advection on CO₂ flux measurements, *Basic Appl. Ecol.*, *1*, 177–188.
- Fassbinder, J., T. Griffis, and J. Baker (2012), Evaluation of carbon isotope flux partitioning theory under simplified and controlled environmental conditions, *Agr. Forest Meteorol.*, *153*, 154–164.
- Fassbinder, J., N. Schultz, J. Baker, and T. Griffis (2013), Automated, low-power chamber system for measuring N₂O emissions, *J. Environ. Qual.*, *42*, 606–614.
- Gregorich, E., P. Rochette, A. V. den Bygaart, and D. Angers (2005), Greenhouse gas contributions of agricultural soils and potential mitigation practices in eastern Canada, *Soil Till. Res.*, *83*, 53–72.
- Griffis, T., J. Baker, S. Sargent, M. Erickson, J. Corcoran, M. Chen, and K. Billmark (2010), Influence of C₄ vegetation on ¹³CO₂ discrimination and isoforcing in the upper Midwest, United States, *Global Biogeochem. Cycles*, *24*, GB4006, doi:10.1029/2009GB003594.
- Groffman, P. M., K. Butterbach-Bahl, R. W. Fulweiler, A. J. Gold, J. L. Morse, E. K. Stander, C. Tague, C. Tonitto, and P. Vidon (2009), Challenges to incorporating spatially and temporally explicit phenomena (hotspots and hot moments) in denitrification models, *Biogeochemistry*, *93*(1–2), 49–77.
- Helliker, B. R., et al. (2004), Estimates of net CO₂ flux by application of equilibrium boundary layer concepts to CO₂ and water vapor measurements from a tall tower, *J. Geophys. Res.*, *109*, D20106, doi:10.1029/2004JD004532.
- Hirsch, A. I., A. M. Michalak, L. M. Bruhwiler, W. Peters, E. J. Dlugokencky, and P. P. Tans (2006), Inverse modeling estimates of the global nitrous oxide surface flux from 1998–2001 rid b-8305-2008, *Global Biogeochem. Cycles*, *20*(1), GB1008, doi:10.1029/2004GB002443.
- <http://edgar.jrc.ec.europa.eu>, (2011), Emission database for global atmospheric research (EDGAR), release version 4.2. <http://edgar.jrc.ec.europa.eu>, 2011, *Tech. rep.*, European Commission, Joint Research Centre (JRC)/Netherlands Environmental Assessment Agency (PBL).
- Kort, E. A., et al. (2008), Emissions of CH₄ and N₂O over the United States and Canada based on a receptor-oriented modeling framework and COBRA-NA atmospheric observations, *Geophys. Res. Lett.*, *35*, L18808, doi:10.1029/2008GL034031.
- Lin, J., C. Gerbig, S. Wofsy, A. Andrews, B. Daube, K. Davis, and C. Grainger (2003), A near-field tool for simulating the upstream influence of atmospheric observations: The Stochastic Time-Inverted Lagrangian Transport (STILT) model, *J. Geophys. Res.*, *108*(D16), doi:10.1029/2002JD003161.
- Marschner, F., (1974), The original vegetation of Minnesota (redraft of the original 1930 edition), *Tech. rep.*, U.S. Department of Agriculture, Forest Service. North Central Forest Experiment Station, St. Paul, MN, USA.
- Miles, N. L., S. J. Richardson, K. J. Davis, T. Lauvaux, A. E. Andrews, T. O. West, V. Bandaru, and E. R. Crosson (2012), Large amplitude spatial and temporal gradients in atmospheric boundary layer CO₂ mole fractions detected with a tower-based network in the U.S. upper Midwest, *J. Geophys. Res.-Biogeo.*, *117*, G01019, doi:10.1029/2011JG001781.
- Millar, N., G. Robertson, P. Grace, R. Gehl, and J. Hoben (2010), Nitrogen fertilizer management for nitrous oxide (N₂O) mitigation in intensive corn (maize) production: An emissions reduction protocol for US Midwest agriculture, *Mitigation and Adaptation Strategies for Global Change*, *15*, 185–204.
- Miller, S. M., et al. (2012), Regional sources of nitrous oxide over the United States: Seasonal variation and spatial distribution, *J. Geophys. Res.*, *117*, D06310, doi:10.1029/2011JD016951.
- Mosier, A., C. Kroeze, C. Nevison, O. Oenema, S. Seitzinger, and O. van Cleemput (1998), Closing the global N₂O budget: Nitrous oxide emissions through the agricultural nitrogen cycle - OECD/IPCC/IEA phase II development of IPCC Guidelines for National Greenhouse Gas Inventory Methodology, *Nutr. Cycling Agroecosyst.*, *52*(2–3), 225–248.
- Muller, C., C. Kammann, J. C. G. Ottow, and H. J. Jager (2003), Nitrous oxide emission from frozen grassland soil and during thawing periods, *J. Plant Nutr. Soil Sci.*, *166*(1), 46–53.
- Outram, F., and K. Hiscock (2012), Indirect nitrous oxide emissions from surface water bodies in a lowland arable catchment: A significant contribution to agricultural greenhouse gas budgets? *Environ. Sci. and Technol.*, *46*, 8156–8163.
- Pattey, E., I. Strachan, R. Desjardins, and J. Massheder (2002), Measuring nighttime CO₂ flux over terrestrial ecosystems using eddy covariance and nocturnal boundary layer methods, *Agric. For. Meteorol.*, *113*, 145–158.
- Peterson, B., et al. (2001), Control of nitrogen export from watersheds by headwater streams, *Science*, *292*(5514), 86–90, doi:10.1126/science.1056874.
- Robertson, G., E. Paul, and R. Harwood (2000), Greenhouse gases in intensive agriculture: Contributions of individual gases to the radiative forcing of the atmosphere, *Science*, *289*, 1922–1925.
- Rochette, P., and N. Eriksen-Hamel (2008), Chamber measurements of soil nitrous oxide flux: Are absolute values reliable? *Soil Sci. Soc. Am. J.*, *72*, 331–342.
- Rover, M., O. Heinemeyer, and E. Kaiser (1998), Microbial induced nitrous oxide emissions from an arable soil during winter, *Soil Biol. Biochem.*, *30*(14), 1859–1865.
- Smith, K., and K. Dobbie (2001), The impact of sampling frequency and sampling times on chamber-based measurements of N₂O emissions from fertilized soils, *Global Change Biology*, *7*, 933–945.
- Smith, K., A. Mosier, P. Crutzen, and W. Winiwarter (2012), The role of N₂O derived from crop-based biofuels, and from agriculture in general, in Earth's climate, *Philos. Trans. R. Soc. London, Ser. B.*, *367*, 1169–1174.
- Stehfest, E., and L. Bouwman (2006), N₂O and NO emission from agricultural fields and soils under natural vegetation: Summarizing available measurement data and modeling of global annual emissions, *Nutr. Cycling Agroecosyst.*, *74*, 207–228.
- USDA (1987), Farm drainage in the United States, *Tech. rep.*, United States Department of Agriculture Miscellaneous Publication 1455.
- USDA-NASS (2013), *Corn: Acreage, Yield, and Production, by County and District, Minnesota, 2011–12*, United States Department of Agriculture-National Agricultural Statistics Service, Washington D. C.
- Wagner-Riddle, C., and G. W. Thurtell (1998), Nitrous oxide emissions from agricultural fields during winter and spring thaw as affected by management practices, *Nutrient Cycling in Agroecosystems*, *52*(2–3), 151–163.
- Wagner-Riddle, C., A. Furon, N. L. McLaughlin, I. Lee, J. Barbeau, S. Jayasundara, G. Parkin, P. Von Bertoldi, and J. Warland (2007), Intensive measurement of nitrous oxide emissions from a corn-soybean-wheat rotation under two contrasting management systems over 5 years, *Global Change Biol.*, *13*(8), 1722–1736, doi:10.1111/j.1365-2486.2007.01388.x.
- Werle, P., R. Mucke, and F. Slemr (1993), The limits of signal averaging in atmospheric trace-gas monitoring by tunable diode-laser absorption-spectroscopy (TDLAS), *Appl. Phys. B-Photophysics and Laser Chem.*, *57*, 131–139.
- Williams, I., W. Riley, M. Torn, J. Berry, and S. Biraud (2011), Using boundary layer equilibrium to reduce uncertainties in transport models and CO₂ flux inversions, *Atmos. Chem. Phys.*, *11*, 9631–9641.
- Zhang, X., X. Lee, T. Griffis, J. Baker, M. Erickson, N. Hu, and W. Xiao (2013), The influence of plants on atmospheric methane in an agriculture-dominated landscape, *Int. J. Biometeorol.*, doi:10.1007/s00484-013-00662-y.

1 Auxiliary Material Submission for Paper 2013GB004620
2 Reconciling the differences between top-down and bottom-up estimates of
3 nitrous oxide emissions for the US Corn Belt
4

5 Timothy J Griffis (Department of Soil, Water, and Climate, University of
6 Minnesota, Saint Paul, Minnesota, USA), Xuhui Lee (School of Forestry and
7 Environmental Studies, Yale University, New Haven, Connecticut, USA),
8 John M. Baker (USDA-ARS and Department of Soil, Water, and Climate,
9 University of Minnesota, Saint Paul, Minnesota, USA), Michael P. Russelle
10 (USDA-ARS and Department of Soil, Water, and Climate, University of
11 Minnesota, Saint Paul, Minnesota, USA), Xin Zhang (Woodrow Wilson School
12 of Public and International Affairs, Princeton University, Princeton New
13 Jersey, USA), Rod Venterea (USDA-ARS and Department of Soil, Water, and
14 Climate, University of Minnesota, Saint Paul, Minnesota, USA), and Dylan
15 B. Millet (Department of Soil, Water, and Climate, University of
16 Minnesota, Saint Paul, Minnesota, USA)
17

18 Griffis, T.J., X. Lee, J.M. Baker, M.P. Russelle, X. Zhang, R. Venterea,
19 and D.B. Millet, Reconciling the differences between top-down and bottom-
20 up estimates of nitrous oxide emissions for the US Corn Belt, Global
21 Biogeochemical Cycles, XX, XXXX-XXXX
22
23

24 Introduction

25 This file provides additional details related to the bottom-up nitrous
26 oxide emission calculations, the tall tower nitrous oxide concentration
27 and flux measurements, nitrous oxide flux measurements from automated
28 chambers, and other literature values of nitrous oxide emissions.
29

30 1. Auxiliary_Information_GBC_2013.doc. This word file describes the
31 methodological details related to the bottom-up nitrous oxide emission
32 estimates and the tall tower nitrous oxide concentration and flux
33 measurements.
34

35 2. TableS1.doc. This word document (Table S1) is to be included within
36 the Auxiliary_Information_GBC_2013.doc. This Table describes estimated
37 synthetic nitrogen fertilizer, livestock populations, and manure-derived
38 nitrogen for the Corn Belt.
39

40 3. FigureS1.pdf. This figure (Figure S1) is to be included with the
41 Auxiliary_Information_GBC_2013.doc. This Figure compares the nocturnal
42 boundary layer budget estimate of CO2 flux with eddy covariance CO2
43 fluxes.
44

45 4. FigureS2.pdf. This figure (Figure S2) is to be included with the
46 Auxiliary_Information_GBC_2013.doc. This Figure shows the nighttime
47 concentration footprint estimate for the tall tower based on the
48 Stochastic Time-inverted Lagrangian Transport (STILT) model.
49

50 5. FigureS3.pdf. This figure (Figure S3) is to be included with the
51 Auxiliary_Information_GBC_2013.doc. This Figure shows the wavelet
52 decomposition for nitrous oxide concentration measurements at the
53 Rosemount tall tower and for other "background" sites.
54

55 6. FigureS4.pdf. This figure (Figure S4) is to be included with the
56 Auxiliary_Information_GBC_2013.doc. This Figure shows the influence of
57 wind direction and air temperature on the tall tower nitrous oxide
58 concentrations measured at 100 m above the ground.

59
60 7. FigureS5.pdf. This figure (Figure S5) is to be included with the
61 Auxiliary_Information_GBC_2013.doc. This Figure shows the mean monthly
62 nitrous oxide flux estimates based on four boundary-layer budget
63 techniques.

64
65 8. FigureS6.pdf. This figure (Figure S6) is to be included with the
66 Auxiliary_Information_GBC_2013.doc. This Figure shows the hourly soil
67 nitrous oxide fluxes measured using an automated chamber system coupled
68 to a tunable diode laser system in a corn/soybean agricultural field.

69
70

1 **Reconciling the differences between top-down and bottom-up**
2 **estimates of nitrous oxide emissions for the US Corn Belt**

3
4 Timothy J. Griffis¹, Xuhui Lee^{2,3}, John M. Baker^{1,4}, Michael Russelle^{1,4}, Xin Zhang⁵, Rod Venterea^{1,4}, Dylan Millet¹

5
6 1. Department of Soil, Water, and Climate, University of Minnesota-Twin Cities

7
8 2. School of Forestry and Environmental Studies, Yale University

9
10 3. Yale-NUIST Center on Atmospheric Environment, Nanjing University of Information Science and Technology,
11 Nanjing, China

12
13 4. United States Department of Agriculture – Agricultural Research Service

14
15 5. Woodrow Wilson School of Public and International Affairs, Princeton University, Princeton New Jersey, USA

16
17
18 Authors for correspondence:

19 Tim Griffis

20 Email: timgriffis@umn.edu

21 Phone: 612.625.3117

22
23 Xuhui Lee

24 Email: xuhui.lee@yale.edu

25 Phone: 203.432.6047

26 **Auxiliary Information**

27

28 **1. Nitrogen inputs**

29 We estimated nitrogen (N) inputs for the Corn Belt based on recent N use and sales statistics provided by
30 the United States Department of Agriculture, Economic Research Service [USDA-ERS, 2011]. For the
31 purpose of N accounting based on sales statistics, we define the Corn Belt by those states with significant
32 corn/soybean land use. These states include: Illinois, Indiana, Iowa, Minnesota, Missouri, Ohio, South
33 Dakota, and Wisconsin. The total area is estimated at 148 million ha. Here agriculture represents
34 approximately 40% of the land use – similar to that in the vicinity of the Minnesota tall tower. These data
35 have been summarized in Table S1. Approximately 5.0 Tg of synthetic N was added to the Corn Belt in
36 2010. The most significant source was associated with corn production.

37

38 An extensive survey of fertilizer use for the State of Minnesota determined that the average N application
39 rate for corn was 157 kg ha⁻¹ (140 lbs acre⁻¹) with a range of 145 to 164 kg ha⁻¹ [Bierman et al., 2012].
40 This rate is in excellent agreement with our estimates for the entire Corn Belt. The patterns of fertilizer
41 application (timing, amount, type) are important for driving bottom-up emission estimates and
42 understanding the patterns of N₂O flux. For Minnesota, the most common fertilizer types were anhydrous
43 ammonia and urea. Results from the fertilizer survey revealed that 45.9% of land managers used
44 anhydrous ammonia while 44.8% used urea. Further complexity is introduced in terms of the timing of
45 nitrogen application, which varies depending on N source and region. In general, anhydrous ammonia
46 was applied 61% of the time in the fall and 28% of the time during spring. Urea was applied 75% during
47 spring and about 10% during fall. The timing and type of N application can have an important impact on
48 N₂O fluxes.

49

50 The major sources of biological N fixation (BNF) for the Corn Belt are derived from soybean and alfalfa.
51 Typical rates of 84 kg N ha⁻¹ and 152 kg N ha⁻¹, respectively have been reported for the Mississippi river
52 basin [Russelle and Birr, 2004]. Our estimates for the Corn Belt based on the 8-digit HUC land use and
53 yield information were 102 kg N ha⁻¹ and 166 kg N ha⁻¹, respectively. Given the number of hectares
54 planted for each of these crops, we estimated a combined BNF of 2.8 Tg N y⁻¹. Further, the amount of N
55 added back to corn systems in the form of aboveground residue was estimated at 2.2 Tg N y⁻¹.

56

57 Using the most recent agricultural census data [USDA-NASS, 2009] we have estimated N inputs in the
58 form of manure [Lorimor et al., 2004] for the Corn Belt (Table S1). Estimates of daily manure N rate per

59 head of livestock were estimated for swine (17.7 kg N y⁻¹), cattle (57.9 kg N y⁻¹), sheep (6.6 kg N y⁻¹),
60 turkey (1.6 kg N y⁻¹), layers (0.43 kg N y⁻¹), broilers (0.35 kg N y⁻¹) and horses (39.7 kg N y⁻¹). Given
61 the estimated populations for each of these species, and assuming that manure is distributed evenly across
62 the agricultural lands, we estimated an N application rate of 46.3 kg N ha⁻¹ y⁻¹ or 2.7 Tg N y⁻¹.

63
64 Finally, we considered N inputs in the form of wet and dry N deposition, using an average flux of 9.1 kg
65 N ha⁻¹ y⁻¹, 1.3 Tg N y⁻¹) [Anderson and Downing, 2006], and local re-deposition [Anderson and
66 Downing, 2006; Burkhart et al., 2005] of N in the form of ammonium and ammonia (NH_x, 12.3 kg N ha⁻¹
67 y⁻¹, 1.8 Tg N y⁻¹).

68 **Table S1.** Estimated synthetic nitrogen fertilizer, livestock populations, and manure-derived nitrogen for
69 the Corn Belt

70

71 **2. Nocturnal Boundary Layer Budget of Carbon Dioxide**

72

73 **Figure S1:** Comparison of the CO₂ nocturnal boundary layer budget and eddy covariance techniques.
74 The solid line is a 7-day running mean of the NBL budget.

75

76

77

78

79

80

81

82

83

84

85

86

87

88

89

90

91

92
93
94
95
96
97
98
99
100
101
102
103
104
105
106
107
108
109
110
111
112
113
114
115
116
117
118
119
120
121
122
123
124
125
126
127
128

3. Nighttime N₂O Concentration Footprint

The nighttime (20:00 to 04:00 hour) concentration footprint was estimated using the Stochastic Time-inverted Lagrangian Transport (STILT) model using data for September 2009 [Lin et al., 2003]. With this analytical approach, we calculated the footprint for each hour by releasing 100 air parcels at the receptor (44°41'19"N, 93°04'22"W, 185 m) and transporting them backward for one night. The figure below shows the averaged footprint during the nighttime, and it indicates that the nighttime concentration measurement at 185 m is strongly influenced by sources within about 120 km of the tall tower.

Figure S2. Concentration footprint of the tall tower determined using the STILT model in September 2009. The color scale represents the log₁₀ footprint, and the unit of the footprint is ppm (μmole m⁻² s⁻¹)⁻¹ (top panel). Cumulative percentage footprint contribution based on the nocturnal STILT analysis (bottom panel).

4. Spatio-temporal variability in N₂O Concentrations

Figure S3. Wavelet analysis of N₂O concentration from select “background” sites and the Rosemount tall tower (100 m level). The wavelet decomposition is used here to extract the seasonal variability (A5, middle panels) and the short-term (hourly) noise (D5, right panels).

Figure S4. Influence of wind direction and air temperature on the tall tower N₂O observations measured at the 100 m level.

129
130
131
132
133
134
135
136
137
138
139
140
141
142
143
144
145
146
147
148
149
150
151
152
153
154
155
156
157
158
159
160
161
162
163
164
165
166
167
168

5. Boundary Layer N₂O Budgets

The mean monthly N₂O emissions for each boundary layer budget technique are shown in Figure S5 and indicate that June, August, and September had the largest mean emissions. Overall, the largest fluxes were observed during the growing season, which is generally consistent with automated soil chamber measurements.

Figure S5: Mean monthly nitrous oxide flux estimates based on the nocturnal boundary layer (NBL), modified Bowen ratio (MBR night and daily), and equilibrium boundary layer (EBL) techniques for 2011. The dashed line shows the ensemble mean. The cross-correlation matrix shows a correlation ranging from 0.47 to 0.80 for the various methods.

6. Automated Soil Chamber N₂O Fluxes

Figure S6. Hourly soil N₂O fluxes measured using an automated chamber system coupled to a tunable diode laser.

7. Other N₂O sources

The upscaling calculations required estimates of other N₂O sources within the footprint of the tall tower. These were based on literature values and included emissions from natural vegetation [Zhuang et al., 2012], urban land use [EDGAR V4.2], and lakes [McCrackin and Elser, 2010; McCrackin and Elser, 2011; Mengis et al., 1997].

8. References

United States Department of Agriculture – Economic Research Service, United States, Fertilizer use and price. *Technical report* 2011, 2011

Bierman P, Rosen C, Venterea R, Survey of nitrogen fertilizer use on corn in Minnesota. *Agricultural Systems* 109: 43–52, 2012

Russelle M, Birr A, Large-scale assessment of symbiotic dinitrogen fixation by crops: Soybean and alfalfa in the Mississippi River Basin. *Agronomy Journal* 96: 1754-1760, 2004

United States Department of Agriculture – National Agricultural Statistics Service, Census of agriculture, 2007. *Technical Report* 2009, 2009

169 Lorimor J, Powers W, Sutton A, Manure characteristics: Manure management systems series, mwps-18,
170 section 1, *Technical report*, Iowa State University, Midwest Plan Service, Iowa State University, Ames,
171 Iowa, 2004
172
173 Anderson K, Downing J, Dry and wet atmospheric deposition of nitrogen, phosphorous and silicon in an
174 agricultural region. *Water, Air, and Soil Pollution* 176: 351–374, 2006
175
176 Burkhart M, Liebman DJM, Herndl C, Impacts of integrated crop-livestock systems on nitrogen dynamics
177 and soil erosion in western Iowa watersheds. *Journal of Geophysical Research-Biogeosciences* 110:
178 G01009, doi:10.1029/2004JG000008, 2005
179
180 Zhuang Q, Lu Y, Chen M, An inventory of global N₂O emissions from the soils of natural terrestrial
181 ecosystems. *Atmospheric Environment* 47: 66-75, 2012
182
183 McCrackin ML, Elser JJ, Atmospheric nitrogen deposition influences denitrification and nitrous oxide
184 production in lakes. *Ecology* 91: 528-539, 2010
185
186 McCrackin ML, Elser JJ, Greenhouse gas dynamics in lakes receiving atmospheric nitrogen deposition.
187 *Global Biogeochemical Cycles* 25: GB4005, 2011
188
189 Mengis M, Gachter R, Wehrli B, Sources and sinks of nitrous oxide (N₂O) in deep lakes. *Biogeochemistry*
190 38: 281-301, 1997
191

1 **Table S1.** Estimated synthetic nitrogen fertilizer, livestock populations, and manure-derived nitrogen for
 2 the Corn Belt

Crop	Area (10⁶ ha)	Rate (kg N ha⁻¹)	Total N (Tg N y⁻¹)
Corn	24.6	142.6	3.5
Soybean	21.8	3.2	0.07
All wheat varieties	3.3	55.7	0.18
Cotton	0.12	77.2	0.009
Other	10.0	122.7	1.2
Total	59.8	-	4.96

3

Type	Population (10⁶)	Rate (kg N animal⁻¹)	Total N (Tg N y⁻¹)
Cattle	27.6	57.9	1.60
Swine	45.0	17.7	0.79
Sheep	1.2	6.6	0.008
Layers	146.5	0.43	0.06
Broilers	477.2	0.35	0.17
Turkey	46.5	1.6	0.07
Horses	0.85	39.7	0.03
Total	744.9	-	2.74

4

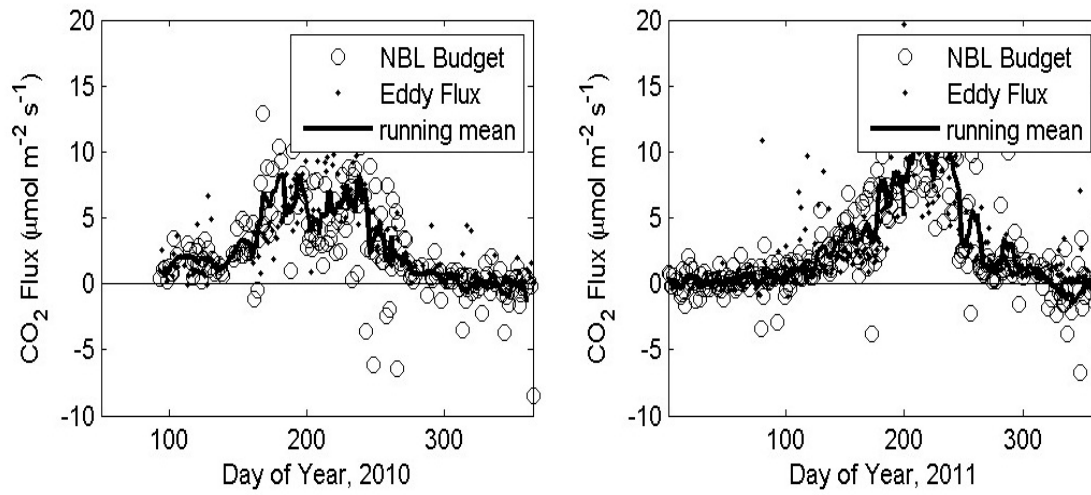


Figure S1: Comparison of the CO₂ nocturnal boundary layer budget and eddy covariance techniques. The solid line is a 7-day running mean of the NBL budget.

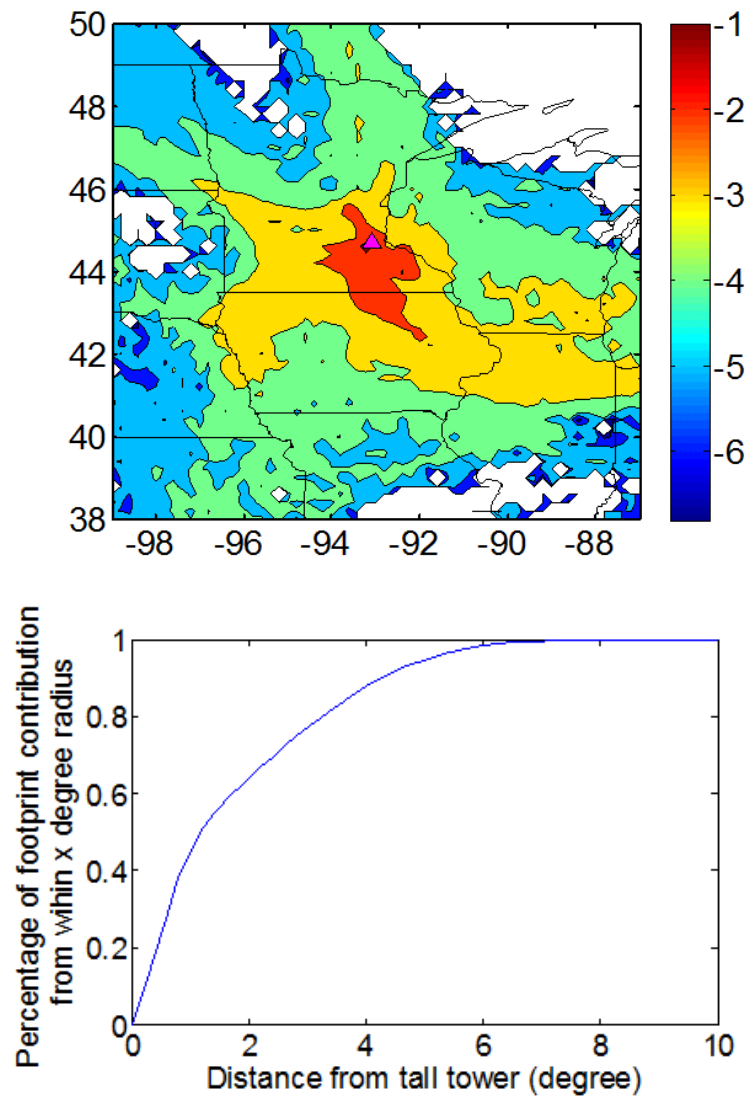


Figure S2. Concentration footprint of the tall tower determined using the STILT model in September 2009. The color scale represents the log10 footprint, and the unit of the footprint is ppm ($\mu\text{mole m}^{-2} \text{s}^{-1}$)⁻¹ (top panel). Cumulative percentage footprint contribution based on the nocturnal STILT analysis (bottom panel).

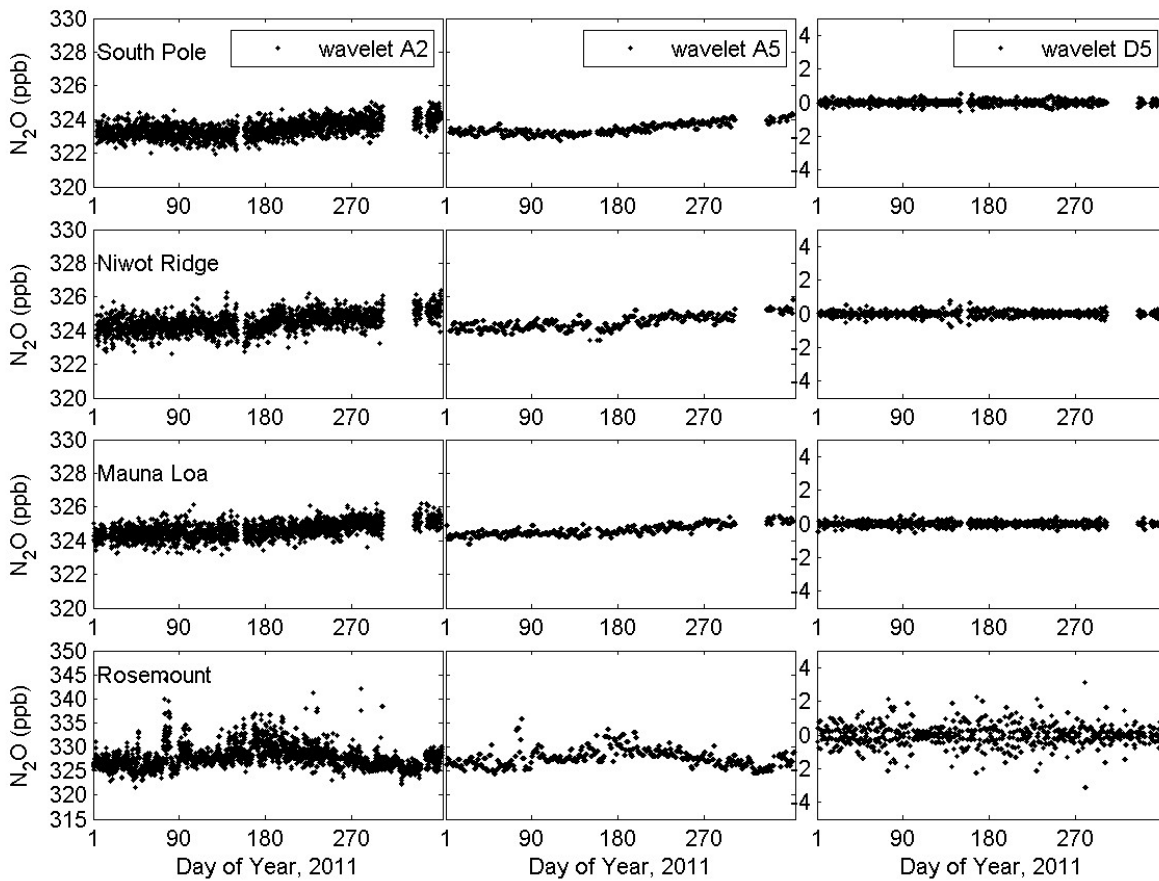


Figure S3. Wavelet analysis of N_2O concentration from select “background” sites and the Rosemount tall tower (100 m level). The wavelet decomposition is used here to extract the seasonal variability (A5, middle panels) and the short-term (hourly) noise (D5, right panels).

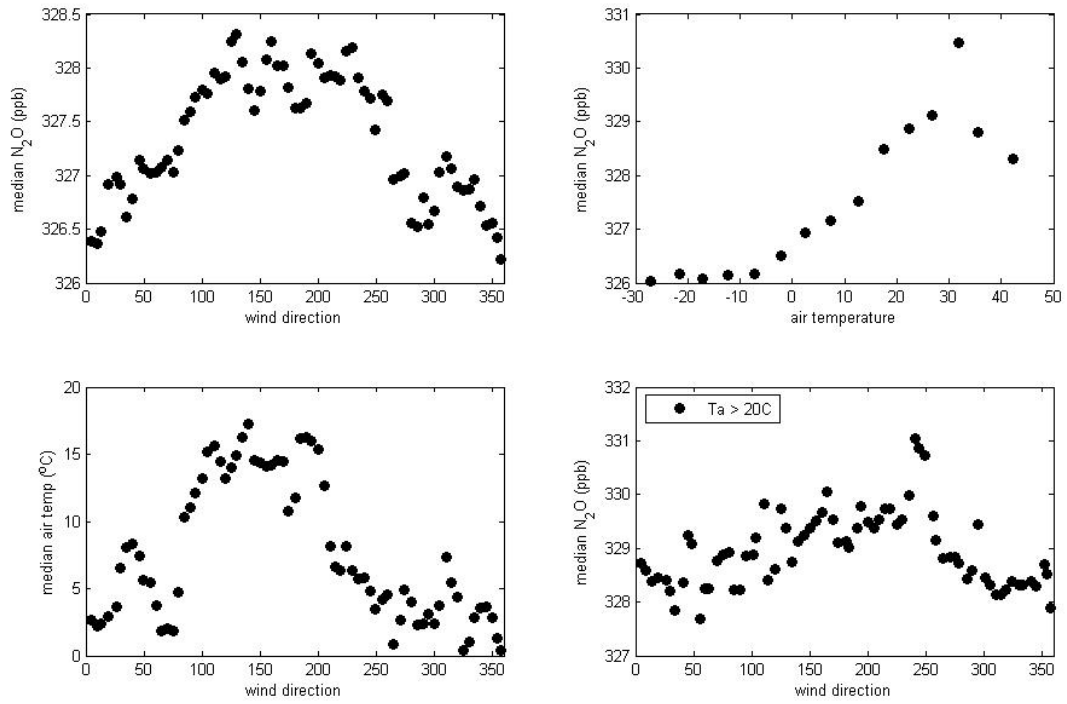


Figure S4. Influence of wind direction and air temperature on the tall tower N₂O observations measured at the 100 m level.

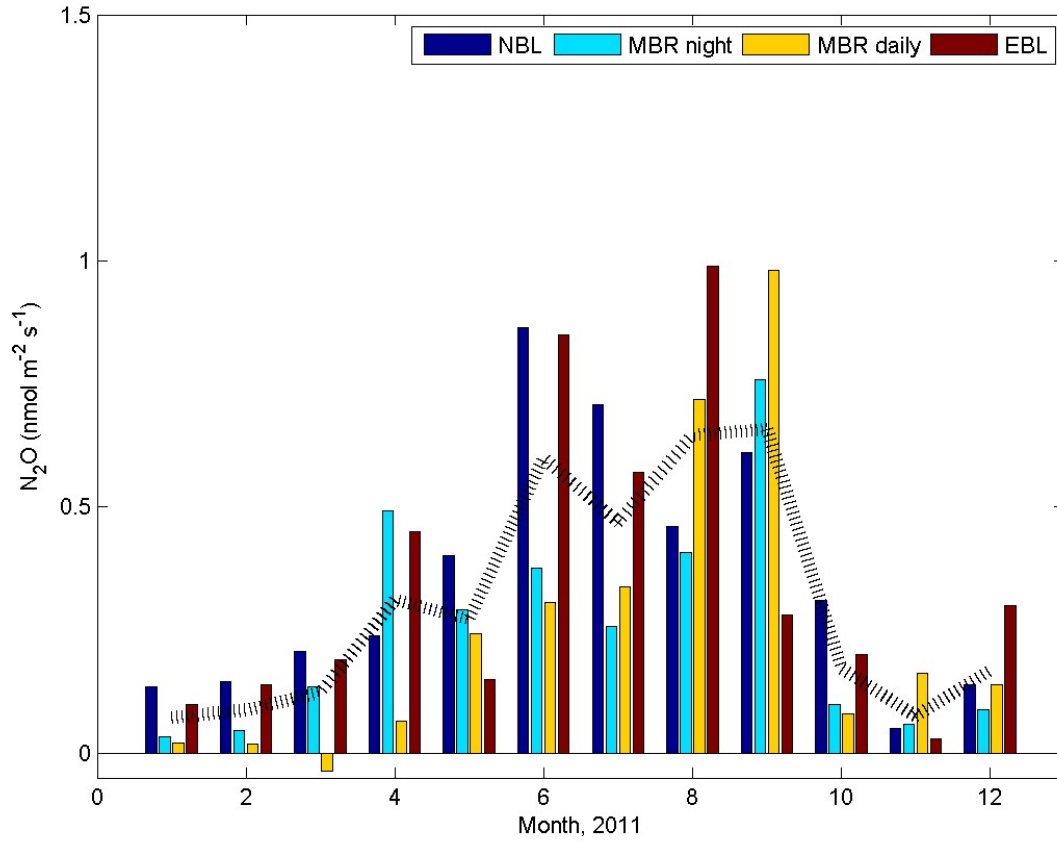


Figure S5: Mean monthly nitrous oxide flux estimates based on the nocturnal boundary layer (NBL), modified Bowen ratio (MBR night and daily), and equilibrium boundary layer (EBL) techniques for 2011. The dashed line shows the ensemble mean. The cross-correlation matrix shows a correlation ranging from 0.47 to 0.80 for the various methods.

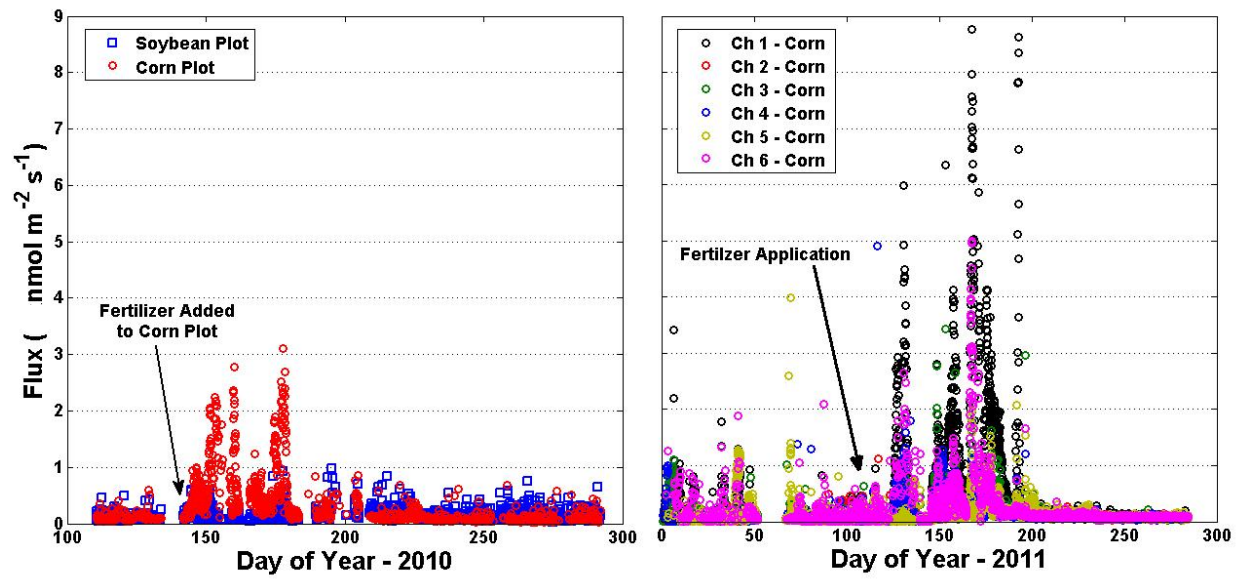


Figure S6. Hourly soil N₂O fluxes measured using an automated chamber system coupled to a tunable diode laser.